The main nitrate transporter of the dinoflagellate *Lingulodinium polyedrum* is constitutively expressed and not responsible for daily variations in nitrate uptake rates

Steve Dagenais Bellefeuille and David Morse*

Institut de Recherche en Biologie Végétale,

Département de Sciences Biologiques,

Université de Montréal, Montréal, Québec, Canada

H1X 2B2

* Author to whom correspondence should be addressed

Key Words: *Lingulodinium polyedrum*, nitrate transporters, NRT2, nitrate uptake, diurnal rhythm, circadian clock

Abstract

Dinoflagellates are unicellular eukaryotes capable of forming spectacular harmful algal blooms (HABs). Eutrophication of coastal waters by fertilizer runoff, nitrate in particular, has contributed to recent increases in the frequency, magnitude and geographic extent of HABs. Although physiological nitrate uptake and assimilation in dinoflagellates have often been measured in the field and in the laboratory, no molecular components involved in nitrate transport have yet been reported. This study reports the first identification and characterization of dinoflagellate nitrate transporters, found in the transcriptome of the bloom-forming *Lingulodinium polyedrum*. Of the 23 putative transporters found by BLAST searches, only members of the nitrate transporter 2 (NRT2) family contained all key amino acids known to be essential for nitrate transport. The dinoflagellate NRT2 sequences have 12 predicted transmembrane domains, as do the NRT2 sequences of bacteria, plants and fungi. The NRT2 sequences in *Lingulodinium* appear to have two different evolutionary origins, as determined by phylogenetic analyses. The most expressed transcript of all putative nitrate transporters was determined by RNA-Seq to be LpNRT2.1. An antibody raised against this transporter showed that the same amount of protein was found at different times over the light dark cycle and with different sources of N. Finally, global nitrate uptake was assessed using a ^{15}N tracer, which showed that the process was not under circadian-control as previously suggested, but simply light-regulated.

1. Introduction

Dinoflagellates are unicellular eukaryotes found in most marine and freshwater ecosystems. While members of this group contains important primary producers and, in the case of the genus *Symbiodinium*, are essential for the survival of tropical reef corals (Davy et al., 2012), dinoflagellates are also infamous because some species can form harmful algal blooms (HABs). These blooms can cause illness or death to aquatic wildlife, damaging ecosystems and negatively impacting tourism and fish industries. Public health is also threatened by toxic blooms, because human consumption of toxin-contaminated seafood can result in intoxication or even death in extreme cases. Some HAB species, such as *Karenia brevis* in the Gulf of Mexico, secrete neurotoxins that have an airborne component and can mix with marine aerosols (Pierce et al., 2003). When driven by winds, people onshore inhaling the toxic sea spray can suffer severe respiratory irritations. Thus, it is a growing concern that HAB events have globally increased in frequency, magnitude and geographic extent over the last 40 years (Anderson et al., 2012). It also justifies the heightened attention scientific and governmental authorities are giving to research on bloom dynamics and the causes leading to HAB expansions (Anderson et al., 2012).

While bloom formation and its persistence involve a complex interplay of biotic and abiotic factors (Anderson et al., 2012), increases in nutrients, particularly phosphorus (P) and nitrogen (N), has often been positively correlated with HABs in various coastal regions of the world (Anderson et al., 2008; Bodeanu and Ruta, 1998; Okaichi, 1997). A recent example is the Changjiang River in China where agricultural runoffs have contributed to a dramatic ~ 400% increase in nitrate concentration between 1960s and 2004, while phosphate concentration increased by ~ 30% between 1980s and 2004 (Zhou et al., 2008). As a result, in a 20 year-period there was a ~ 4-fold augmentation in phytoplankton standing stocks. Also during the same period, the initially diatom-dominated communities started to shift toward dinoflagellates, which is consistent with the observation that diatoms are poor competitors to flagellates when the N: P

ratio is high (Egge, 1998). The most striking consequence of the Changjiang eutrophication was the difference in number of reported HABs in the adjacent coastal waters of the East China Sea, that passed from 2 events before 1980s to ~ 30-80 HABs per year between 2001 and 2005 (Zhou et al., 2008). Because these recent HABs are mainly caused by photosynthetic dinoflagellates (Zhou et al., 2008), these organisms must have very efficient ways in utilizing nitrate for rapid proliferation.

Since nitrate is the most abundant form of bioavailable N in most aerobic soils and marine environments (Crawford and Forde, 2002; Gruber, 2008), its uptake is expected to control the majority of N that can be assimilated for most organisms. This explains the intensive effort over the past several decades to isolate and characterize the genes responsible for nitrate transport in many phylogenetic groups, including bacteria (Moir and Wood, 2001), fungi (Unkles et al., 1991; Unkles et al., 2001), and green plants (Krapp et al., 2014; Tsay et al., 2007). The alveolates, among which are found the dinoflagellates, are a noteworthy exception. The rationale for the molecular characterizations is that nutrient uptake results from the combined action of multiple transporters each with particular enzymatic kinetics, regulation patterns and crosstalk, and that once transporter properties are defined, an overall system can be developed to help in the predictions of an organism's behaviour under fluctuating nutrient conditions. Thus, characterization of dinoflagellate nitrate transporters could complement physiological and field studies in understanding how N uptake influences HABs.

Four gene families have been shown to possess nitrate transport activity in eukaryotes: the nitrate transporter 1/ peptide transporter (NPF) (previously NRT1/PTR), the nitrate transporter 2 (NRT2) of the major facilitator superfamily (MFS), the chloride channels (CLCs) and the slow anion channel-associated 1 homologues (SLAC1/SLAH) (Krapp et al., 2014). Although not working as a transporter alone, nitrate assimilation related (NAR2) is a small protein that directly

interacts with several NRT2 (Kotur et al., 2012; Orsel et al., 2006). The NAR2 protein stimulates nitrate uptake of all seven *Arabidopsis* NRT2 (Kotur et al., 2012), and interaction is mandatory for NRT2.1 of the green alga *Chlamydomonas reinhardtii* where nitrate-elicited currents are only detected when both proteins are co-expressed in *Xenopus* oocytes (Zhou et al., 2000a). In contrast, a well characterized NRT2 from the fungus *Aspergillus nidulans* (NrtA, previously CrnA), functions without NAR2 (Zhou et al., 2000b). Members of the NPF and NRT2 families can be found in all kingdoms of life (Leran et al., 2014), except for animals that lack NRT2 proteins (Slot et al., 2007). The CLCs are also ubiquitous in nature (Jentsch, 2008), but nitrate transport has only been demonstrated for two members, both found in *Arabidopsis* (De Angeli et al., 2006; von der Fecht-Bartenbach et al., 2010). The AtCLC-a protein was shown to be a nitrate/proton antiporter involved in the accumulation of nitrate into the plant tonoplast (De Angeli et al., 2006), while AtCLC-b showed a similar activity after heterologous expression in *Xenopus* oocytes (von der Fecht-Bartenbach et al., 2010). The proteins AtSLAC1 and AtSLAH3 also displayed nitrate transport activity when expressed in oocytes (Geiger et al., 2011; Geiger et al., 2009), but they are the only members of the SLAC1/SLAH family that possess this function. These observations suggest that dinoflagellate nitrate transporters are more likely to belong to the NPF and NRT2 families than to the CLCs or SLAC1/SLAH.

The non-toxic marine dinoflagellate *Lingulodinium polyedrum* forms HABs along the Southern California coast (Kudela and Cochlan, 2000; Lewis and Hallet, 1997). Success of this organism during the upwelling season was attributed in part to its ability to migrate into nitrate-rich subsurface waters at night and assimilate nitrate in the dark (Harrison, 1976). Curiously, nitrate uptake was found to have a strong diel rhythmicity, with the peak observed in the middle of the day (Harrison, 1976). Furthermore, a circadian peak in nitrate reductase (NR) activity was also found during the day (Ramalho et al., 1995). It has been suggested that nitrate uptake could

be controlled by an endogenous clock in *Lingulodinium* (Roenneberg and Rehman, 1996), but experimental data supporting this hypothesis has not yet been reported. Thus, the first aim of this study was to test for circadian nitrate uptake for *Lingulodinium* grown in constant light. The second aim was to identify putative dinoflagellate nitrate transporters from a recently published *Lingulodinium* transcriptome database (Beauchemin et al., 2012) and to characterize the most promising candidates. The final aim was to test the hypothesis that changes in nitrate uptake rates resulted from changes in transporter levels.

2. Material and methods

2.1 Cell culture

2.1.1 Initial conditions

Unialgal but not axenic *Lingulodinium polyedrum* (CCMP 1936, previously *Gonyaulax polyedra*) was obtained from the Provasoli-Guillard National Center for Marine Algae and Microbiota (East Boothbay, ME, USA). For all experiments, cell cultures were initially grown in normal f/2 medium prepared using Instant Ocean under 12 h light (40 µmol photons m^{-2} s^{-1} cool white fluorescent light) and 12 h darkness at a temperature of 18 ± 1 °C. Cells were harvested by filtration on Whatman 541 paper and stored at -80 ºC until use.

2.1.2 Daily and circadian nitrate uptake measurements

Nitrate uptake was monitored using a stable isotope analysis. Culture aliquots were spiked with ^{15}N-labeled $NaNO_3^-$ (98 atom % ^{15}N, Sigma-Aldrich) at different times during a light dark cycle (ZT; Zeitgeber times) or during constant light (CT; Circadian times) for 1 h durations. In the first experiment (ZT), cultures were grown under a 12:12 light/dark regime, with ZT0

corresponding to lights on and ZT12 to lights off. In the second experiment (CT), cultures were grown in continuous light for two days, with $Na^{15}NO_3^-$ incubations and cell harvests made on the second day. For both experiments, cell cultures were filtered on Whatman 541 filters and transferred to an f/2 medium supplemented with half the amount of $NaNO_3^-$ normally included in this medium (normal concentration = 880 µM). These ~ 1.5 L cultures were divided into multiple 150 ml aliquots and incubated under light dark or constant light conditions. $Na^{15}NO_3^-$ was added to the cultures to a final concentration of 440 µM at different times and cells were harvested 1 h later. Data are reported as $\delta\ ^{15}N$, which represent the ^{15}N: ^{14}N ratio in cells after one hour of ^{15}N accumulation relative to the same ratio in atmospheric air. In these experiments, specific nitrate uptake rates (V) were not calculated because the amount of ^{15}N used as a source was higher than levels accepted by the commercial facility (see below) performing the isotopic analysis. The $\delta\ ^{15}N$ is nonetheless a good approximation of nitrate uptake rates, since all variables except the time of sampling under the LD cycle were held constant. Samples without added ^{15}N have a $\delta\ ^{15}N$ of -5.6 ± 0.1.

2.1.3 Expression of LpNRT2.1 protein

Cell cultures were grown in one of four different media: 1) f/2, which is normally supplemented with 880 µM $NaNO_3$ (f/2+NO_3^-); 2) f/2-N (or N-depleted), which is f/2 lacking added $NaNO_3$; 3) f/2+NO_2^-, which is f/2-N supplemented with 10 µM $NaNO_2$; and 4) f/2+NH_4, which is f/2-N supplemented with 40 µM NH_4Cl. To compare cell growth in media with different N, normal f/2 cultures were filtered on Whatman 541 paper, washed with 200 ml of f/2-N medium and resuspended in f/2-N. After resuspension, the 1.5 L flasks were divided into multiple 200 ml aliquots and $NaNO_3$, $NaNO_2$ and NH_4Cl was added to the final concentrations listed above. All cultures were harvested after 2 h or 24 h hour of growth in their respective medium.

2.2 Stable isotope analysis

Measurement of $\delta^{15}N$ (expressed as ‰ relative to air) was performed using a continuous flow Isoprime 100 TM coupled to a Vario Micro CubeTM elemental analyzer (at Geotop-UQAM, Montreal, PQ, Canada). The analytical step was preceded by a preparative step, where harvested cells were lyophilized, weighed and inserted into tin capsules.

2.3 BLAST searches, phylogeny and bioinformatic analyses

Protein sequences encoding putative nitrate transporters in *Lingulodinium* were selected based on their homology to reported nitrate transporters in *Arabidopsis thaliana*: AtNRT2.1; AEE28241, AtNAR2.1; CAC36292, AtNPF6.3 (CHL1); AEE28838, AtCLC-a; AED94612, and AtSLAC1; NP_563909 (Krapp et al., 2014). The TBLASTN analyses were performed against the Transcriptome Shotgun Assembly (TSA) database of *Lingulodinium polyedrum* (taxid: 160621) using default parameters. Hits with e-values ≤ -20 were selected and a second BLAST search was made using these hits against the *Lingulodinium* TSA database to eliminate redundant sequences. Presence of complete open reading frames (ORF) for the NRT2 sequences was confirmed by PCR-amplifications of a Rapid Amplification of cDNA Ends (RACE) (Clontech) library, insertion in pUCm-t vectors (Bio Basic), and Sanger sequencing. Stop codons in frame with the longest ORF were found in both the 5'- and 3'-UTRs for all NRT2 sequences.

Phylogenetic analysis was performed using RAxML (Stamatakis, 2014), which is available online at the CIPRES science gateway (Miller et al., 2010). The NRT2 sequences were aligned with ClustalW, imported in PHYLIP format into CIPRES and analysed with RAxML-HPC Blackbox using default parameters. The tree was visualized using dendroscope (Huson and Scornavacca, 2012). Major taxonomic groups used for classification are reported in the Tree of Life Web Project (ToL).

Analysis of amino acids essential for NRT2 activity was based on site-directed mutagenesis studies using the NrtA of *Aspergillus nidulans* (Kinghorn et al., 2005; Unkles et al., 2012; Unkles et al., 2004). The NrtA sequence was compared using ClustalW-alignment to all NRT2 sequences from *Lingulodinium* and one sequence for each group of organisms presented in the phylogeny. The nitrate signature (NS) motif has been previously described by (Unkles et al., 2004) and (Forde, 2000).

Transmembrane domains (TM) and topologies were predicted using TMHMM (Krogh et al., 2001), TMPred (Hofmann and Stoffel, 1993) and TopPred (Claros and von Heijne, 1994; von Heijne, 1992). TMHMM version 1 and TMPred were run on default parameters, while TopPred version 1.10 was run with all parameters at default settings except for the organism type, which was set to “eukaryot” instead of “prokaryot” and the wedge window size (-q), which was set to 3 instead of 5.

2.5 Relative transcript abundance of Lingulodinium NRT2 sequences

Reads Per Kilobase per Million mapped reads (RPKM) values for putative nitrate transporters were obtained from a published transcriptomic study in *Lingulodinium polyedrum* (Roy et al., 2014a). The RPKM data were generated after mapping raw reads from two different RNA-Seq experiments onto a Trinity (Roy et al., 2014b) or a Velvet (Beauchemin et al., 2012) assembly. RPKM data from eight samples were combined and used to compare the relative transcript abundance of the putative nitrate transporters since there was no difference in transcript levels for any gene between the different samples (Roy et al., 2014a).

2.6 Electrophoretic analyses

Samples for 1D electrophoresis were prepared from 10 mg of cells mechanically lysed 2 min in a bead beater (BioSpec products) at 4°C with 10 mM Tris, pH 8.0; 1 mM EDTA and 1 mM PMSF. SDS sample buffer (final concentration: 50 mM Tris-HCl pH 6.8; 2% SDS; 100 mM DTT; 10 % glycerol) was added to the cell lysates and boiled 10 min at 95°C. 10 µL of each sample was electrophoresed on 10% polyacrylamide gels.

Samples for 2D electrophoresis were prepared from 200 mg of cells mechanically lysed 2 min in a bead beater at 4°C with 7M urea and 2M thiourea. 4% CHAPS was added after lysis and cell solutions were desalted on Bio-Rad Econo-Pac® 10DG columns following the manufacturer's instructions. 200 µg of proteins were resuspended in 125 µl of rehydration buffer (7M urea; 2M thiourea; 4% CHAPS; 20 mM DTT; 0.2% Bio-Rad's Bio-Lyte Ampholyte pH 4-7) and applied to 7 cm ReadyStrip ™ IPG isoelectric focusing (IEF) strips from Bio-Rad. Strips were allowed to rehydrate passively for 14 h before IEF, which was performed at 4000 V for 150 min with Rapid Ramp at 20°C. After IEF, strips were equilibrated 10 min in 2.5 ml of SDS equilibration buffer I (6M urea; 0.375 M Tris-HCl, pH 8.8; 2% SDS; 20% glycerol; 2% DTT), and 10 min in 2.5 ml of SDS equilibration buffer II (6M urea; 0.375 M Tris-HCl, pH 8.8; 2% SDS; 20% glycerol; 2.5% iodoacetamide). Second-dimension electrophoresis was carried on 10% polyacrylamide gels.

For Western analysis, 1D and 2D gels were transferred to nitrocellulose using a wet electroblotting system. The protein blots were blocked with 2.5% powdered milk and 2.5% BSA in Tris-buffered saline containing 0.05% Tween 20. Membranes were incubated overnight at 4°C with either a 1:1000 dilution of mouse anti-NRT2.1 or a 1:10000 dilution of rabbit anti-Rubisco to control for protein loading (Nassoury et al., 2001). The anti-NRT2.1 is a monoclonal antibody against the epitope GKNDADSPTD produced in mice ascites by Abmart (NJ, USA). This peptide was unique to the NRT2.1 sequence when tested with BLAST against the *Lingulodinium* TSA

database. The epitope is in a predicted soluble domain near the N-terminal. Protein bands or spots had a size and pI similar to the theoretical values, 60 kD and 6.4 respectively, calculated for LpNRT2.1 using the Compute pI/Mw tool available on the ExPASy portal (Gasteiger et al., 2003). Antibody binding was visualized by using a 1:10000 dilution of commercial peroxidase-linked secondary antibodies against mouse (GenScript) or rabbit (Amersham Pharmacia Biotech) and chemiluminescence (HyGLO, Denville Scientific Inc). An ImageQuant LAS 4000 was used for imagery and pictures were modified for contrast only using Adobe Photoshop 8.0.

2.8 Statistical analysis

Results in figure 1 (n=3) and figure 2 (n=8) are presented as means ± SE. An analysis of variance was used to test for statistical significance using the JMP software (SAS).

3. Results

To establish the patterns of nitrate uptake by *Lingulodinium* in light dark and constant light conditions, a stable isotope analysis was performed using a ^{15}N tracer. While *Lingulodinium* was still capable of taking nitrate in the dark, all $\delta\ ^{15}N$ values measured during the day were consistently higher than those measured during the night (Fig. 1A). Nitrate uptake was highest at the beginning of the day followed by a gradual decline during the rest of the day (Fig. 1A). Interestingly, the marked changes in nitrate uptake observed at the transitions between light and dark phases argued that nitrate uptake was more likely to be light dependent than circadian-regulated. To test this, the ^{15}N experiment was repeated under constant light (Fig. 1B). No significant changes in $\delta\ ^{15}N$ were observed over an entire circadian cycle (Fig. 1B) confirming the process is light dependent. The observation that the total amount of $\delta\ ^{15}N$ taken up during a 24-h

period in light dark and constant light conditions is similar (Supp. Fig. S1) suggests the ability of *Lingulodinium* to store N in an intracellular nitrate pool may be limited.

Next, a list of putative nitrate transporters in *Lingulodinium* was generated by searching the transcriptome with reported nitrate transporters in *Arabidopsis thaliana* (Table 1) (Krapp et al., 2014). In contrast to *Arabidopsis*, where 53 members of the NPF protein family were identified (Tsay et al., 2007), only one NPF sequence was found in *Lingulodinium* and its transcripts were only found in cysts (Roy et al., 2014b). Because all ^{15}N experiments were performed on swimming (nonencysted) cells, it is unlikely that this NPF contributed to the nitrate uptake presented in figure 1. There are 17 *Lingulodinium* sequences with homology to AtCLC-a, but again it seems unlikely that these are specialized for nitrate uptake, because in 15 of them a proline residue, P^{160}, necessary for nitrate selectivity in AtCLC-a and AtCLC-b (Bergsdorf et al., 2009; Wege et al., 2010), was replaced by a serine (Supp. Fig. S2), a modification also observed in mammalian CLC isoforms (Bergsdorf et al., 2009; Wege et al., 2010). Of the 2 remaining sequences, one had a glycine instead of a serine and the other sequence was incomplete and could not be aligned in the region encompassing the selectivity filter. Unsurprisingly, no homologous sequences to the plant guard cell protein SLAC1 were found in *Lingulodinium*. The NAR2 sequences were also missing.

Lastly, *Lingulodinium* also expresses 5 sequences encoding putative nitrate transporters of the NRT2 family (Table 1). All of these transcripts were found in ZT and CT, again without significant variation in either light condition (Roy et al., 2014a) (Fig. 2, S3). The mRNA levels of one NRT2, named LpNRT2.1, were much greater than all the other putative nitrate transporters in table 1, when using either a Trinity (Fig. 2) or a Velvet (Fig. S3) assembly. Thus, NRT2 sequences, in particular LpNRT2.1, were judged the most likely candidates to be involved in nitrate transport. Two NRT2s, JO716588 and JO704794, were omitted in the following analyses,

because their sequences were incomplete in the transcriptome and multiple attempts to amplify their cDNA ends failed.

To assess the evolutionary history of dinoflagellate NRT2, sequences from taxa that rely on this transporter family for nitrate uptake were used for molecular phylogenetic reconstructions (Fig. 3). While distant relationships were poorly supported, monophyly of the major ToL taxonomic groups were respected except for the Hacrobia (cryptophytes and haptophytes). Interestingly, *Lingulodinium* LpNRT2.3 and the NRT2 of the haptophyte (Hacrobia) *Emiliania huxleyi* both clustered together with the green plants and not with their respective groups. Thus, there are at least two different origins for the NRT2 family members in *Lingulodinium*.

The NrtA protein in *Aspergillus nidulans* was the first characterized NRT2 (Unkles et al., 1991) and site-directed mutagenesis studies of this transporter have identified a number of residues that are required for nitrate/nitrite transport (Kinghorn et al., 2005; Unkles et al., 2012; Unkles et al., 2004). All these essential residues were found in *Lingulodinium* NRT2 members and a representative from each of the taxonomic groups used in figure 3 (Fig. 4). Furthermore, *Lingulodinium* NRT2s also contain the two characteristic nitrate signature (NS) motifs. Lastly, the predicted membrane topology and the placement of the essential residues and conserved motifs (F47 in TM1, R87 in TM2, R368 in TM8, NS1 after TM4 and NS2 close to TM11) within this topology (Unkles et al., 2012), was also conserved for the dinoflagellate sequences (Fig. 5). Predictions of membrane topology for the LpNRT2s showed that the $N_{cytosolic}$: $C_{cytosolic}$ organisation, with generally 12 TMs, was also predicted in *Aspergillus*, *Arabidopsis* and other dinoflagellates (Fig. 5). These predictions were in agreement with previous reported models of membrane topologies for NRT2 in fungi, plants and bacteria (Forde, 2000; Kinghorn et al., 2005; Trueman et al., 1996). Taken together, these results thus support the identification of *Lingulodinium* NRT2s as *bona fide* NRT2 involved in nitrate/nitrite transport.

Because the transcript abundance of LpNRT2.1 suggested it may be the most highly expressed member of the NRT2 family, a monoclonal antibody was prepared to assess expression of the protein under different conditions (Fig. 6). Protein expression was first measured at regular intervals during a light dark cycle, which showed no difference at any ZT (Fig. 6A). Thus, changes in protein abundance of LpNRT2.1 cannot account for the difference in nitrate uptake observed between day and night in ZT (Fig. 1A). The possibility that post-translational modifications (PTM) such as phosphorylation could modify LpNRT2.1 and change its activity between day and night was next tested using two-dimensional gel electrophoresis (Fig. 6B). While multiple isoforms were detected, similar to many other dinoflagellate proteins, no difference in the number, intensity or the position of these spots was observed between ZT6 and ZT18 (Fig. 6B). Thus, it seems unlikely that PTM of LpNRT2.1 or/and a particular isoform of the transporter were responsible for the variation in nitrate uptake rates observed in figure 1A.

In addition to being important nutrients, nitrate, nitrite and ammonium have been shown to serve as signalling molecules capable of regulating expression of multiple nitrate transporters and nitrate assimilation enzymes (Glass et al., 2002; Krapp et al., 2014; Wang et al., 2007). Thus, the nutrients themselves are used as signals to control their own uptake and assimilation by the cells. Responses to these nutrients were reported to be extremely rapid (within minutes) in certain cases, and for many proteins, the changes were also transient (Glass et al., 2002; Krapp et al., 2014). For these reasons, the amount of LpNRT2.1 in *Lingulodinium* cells was assayed over a short (2 h) or a longer (24 h) duration in cultures exposed to different sources of N. No variation in protein abundance was detected under any treatments, including N deprivation, at either time (Fig. 6C). Taken together, these results indicated that LpNRT2.1 was the main component of a constitutive nitrate uptake system.

4. Discussion

This study has estimated nitrate uptake rates over a 24-h period and identified potential nitrate transporters in the bloom-forming dinoflagellate *Lingulodinium polyedrum*. Of the 5 classes of putative nitrate transporters found in the *Lingulodinium* transcriptome (Table 1), only proteins of the NRT2 family appear likely to be genuinely involved in nitrate transport (Fig. 4, 5, S2). Five NRT2 sequences were found in the *Lingulodinium* transcriptome, a number similar to the 6 NRT2s reported in the genome of *Chlamydomonas* (Fernandez and Galvan, 2007) and the 7 NRT2s in *Arabidopsis* (Krapp et al., 2014). *Lingulodinium* did not contain any NAR2 sequences, in contrast to plants and green algae (Table 1). It is possible that the NRT2/NAR2 interaction is a particularity of the green lineage, and thus, as is the case with *Aspergillus* NrtA (Zhou et al., 2000b), the NRT2s in *Lingulodinium* may function alone. It is also possible, however, that a *Lingulodinium* NAR2 was not detected by BLAST searches because of low sequence homology. For example, NAR2 in the green algae *Chlamydomonas* shares only 28% identities and 56% coverage (e-value of 0.17) with its homolog in the higher plant *Arabidopsis* NAR2.1. *Lingulodinium* did contain a single NPF family member, although this was expressed only in cysts and not in motile cells (Fig. 2). This is a major difference compared to the abundant and widely distributed NPF sequences found in plants (Leran et al., 2014). In contrast, the green algae *C. reinhardtii* and *Ostreococcus tauri* have only a single uncharacterized NPF each (Derelle et al., 2006; Fernandez and Galvan, 2007), so expansion of the NPF family may be specific to higher plants.

In general, the NRT2 phylogeny supported the monophyly of the major taxonomic groups (Fig. 3), and is consistent with another NRT2 phylogeny, which, although more exhaustive, did not contain sequences from the Hacrobia and Alveolates (Slot et al., 2007). Interestingly, the

NRT2.3 of *Lingulodinium* clustered with the green plants instead of with the other dinoflagellate NRT2 sequences (Fig. 3). This difference is also reflected in the structure, as unlike the other dinoflagellate NRT2s, LpNRT2.3 lacked the long extension between TM1 and TM2, and was thus structurally more similar to *Arabidopsis* NRT2.5 (Fig. 5). Lastly, the expression level of LpNRT2.3 was ~10-fold and ~100-fold less than LpNRT2.2 and LpNRT2.1, respectively (Fig. 2). It seems likely that LpNRT2.3 may have been acquired by horizontal gene transfer.

Comparison of *Lingulodinium* NRT2s with *Aspergillus* NrtA confirmed that the dinoflagellate transporters analysed contained all amino acid residues known to be essential for nitrate/nitrite transport (Fig. 4). Functionally, Arg^{87} and Arg^{368} were shown to be the substrate-binding sites in NrtA (Unkles et al., 2004), and 3D modelling of this transporter predicted that Asn^{459} and Asn^{168} would also be involved in nitrate transport. Indeed, the Asn residues were observed to lie on opposite sides of the probable substrate translocation pore in close proximity to Arg^{87} for Asn^{459} and Arg^{368} for Asn^{168} (Unkles et al., 2012). Six conserved glycine residues, mostly localized within the two repeated motifs NS1 and NS2 (boxed in Fig. 4), were found to be essential for structural positioning of helices as well as for close helix packing and flexibility (Unkles et al., 2012). Phe^{47}, together with other aromatic residues in TM1, were suggested to either close the translocation pore following substrate binding or alternatively, constrain the flexibility of the long side chains of Arg^{87} and Arg^{368} (Kinghorn et al., 2005). In addition, all of these residues and motifs in dinoflagellate NRT2s were localized in regions with the same topology as those of *Aspergillus* NrtA or *Arabidopsis* NRT2.5 (Fig. 5). This suggests positioning of helixes and of the substrate translocation pore in dinoflagellate NRT2s will be similar to that of fungi or plants.

Transit of membrane proteins through the ER in dinoflagellates is not a guarantee that their final destination will be at the plasma membrane. Indeed, nuclear-encoded plastid proteins

in *Lingulodinium polyedrum* were shown to reach the triple-membrane bound chloroplasts via Golgi-derived vesicles and used a leader sequence different from what is typically observed in plants and green algae (Nassoury et al., 2003). This leader sequence contained two distinct hydrophobic domains flanking a region rich in hydroxylated amino acids (S/T). The first hydrophobic region acted as a signal peptide and was always followed by an AXA signal peptidase site. The S/T- rich region was a transit sequence capable of targeting a luciferase reporter into chloroplasts of transgenic plants expressing the construct. Finally, the second hydrophobic domain acted as a stop-transfer signal that anchored plastid proteins in vesicles en route through the Golgi to the chloroplasts. The NRT2 N-terminus does thus not possess the characteristics expected for a plastid-targeted protein. An alternative destination accessible from the Golgi is the vacuole, but no vacuolar targeting signals are known in the dinoflagellates. A last possible destination is the plasma membrane, and only one protein, called p43, has been localized to this location biochemically (Bertomeu et al., 2003). Interestingly, the N terminus of p43 and LpNRT2 do show some elements of similarity, notably a hydrophobic region about 50 residues downstream from the N-terminus and numerous charged and hydroxylated amino acids preceding the hydrophobic region. Thus while plausible, confirmation of a plasma membrane location for the transporter will require immunulocalization. It is unfortunate that the monoclonal antibody raised in this study did not detect its epitope on cell sections.

Transcripts of LpNRT2.1 were found to be the most abundant of all putative nitrate transporters identified in this study (Fig. 2) thus motivating the choice of this protein for antibody production (Fig. 6). Although LpNRT2.1 was constitutively expressed throughout a daily cycle (Fig. 6A) or under different N treatments (Fig. 6C), this mode of expression is not unusual for nitrate transporters, and constitutive nitrate uptake systems have long been postulated in plants and green algae (Fernandez and Galvan, 2007; Tsay et al., 2007). Interestingly, *Arabidopsis*

NRT2.5, which was reported as the major contributor to the constitutive nitrate uptake system in roots (Kotur and Glass, 2015), is also the closest *Arabidopsis* homologue to *Lingulodinium* LpNRT2.1. AtNRT2.5, however, was induced by severe nitrate starvation (Lezhneva et al., 2014), while this induction was not observed for LpNRT2.1 in N-free media (Fig. 6C). Ammonium is usually preferred to nitrate by most photosynthetic organisms, because its assimilation requires less energy than nitrate. Thus, ammonium is reported to repress multiple proteins of the nitrate metabolism, including NRT2s (Fernandez and Galvan, 2007; Tsay et al., 2007). In contrast, LpNRT2.1 was unresponsive to ammonium treatment, and a similar resilience was also observed for the *Lingulodinium* NR (Harrison, 1976). Thus, nitrate uptake in *Lingulodinium* appears to rely mainly on a constitutively expressed protein.

Smayda described three classes of dinoflagellates that differed in their nitrogen uptake strategies: growth, affinity or storage (Smayda, 1997). Growth-strategy species were postulated to have high maximal uptake rates (V_{max}) and thus respond to high ambient nutrient levels. Affinity-strategy species were described as having a high competitive advantage in low nutrient concentrations due to low half-saturation constants (K_s), while storage-strategy dinoflagellates are able to grow in nutrient depleted-habitats because they build large intracellular storage pools when ambient nutrient concentrations are high. *Lingulodinium* does not seem to be an affinity-strategist, since a high K_s value for nitrate in this species has already been reported compared to other dinoflagellates or diatoms (Smayda, 1997). It is also unlikely that *Lingulodinium* uses a storage strategy, since cell division immediately ceased when cell cultures growing in f/2 were transferred to N-depleted f/2 media (Dagenais Bellefeuille et al., 2014). The observation that the $\delta\ ^{15}N$ in constant light reached a constant value intermediate to that measured in day-phase *Lingulodinium* cells (Fig. 1) also suggests that nitrate uptake rates may be reduced because of a limited ability to store N. Thus, by elimination, *Lingulodinium* is likely to be a growth-strategist.

This agrees with the observation that this species blooms when natural N concentrations are elevated (Kudela & Cochlan, 2000).

Daily changes in nitrate uptake, as observed here for *Lingulodinium polyedrum* (Fig. 1A) and previously (Harrison, 1976) are also well documented in plants (Clement et al., 1978; Macduff et al., 1997; Peuke and Jeschke, 1998). In *Arabidopsis*, tobacco and tomato, mRNA expression of NRT2s show a diurnal pattern that correlated with the diurnal uptake of nitrate (Lejay et al., 1999; Matt et al., 2001; Ono et al., 2000). It is clear, however, that no such correlation was found for *Lingulodinium* NRT2.1, where protein levels remained constant for the daily cycle (Fig. 6A). Moreover, no difference in the 2D gel pattern of LpNRT2.1 was detected between day and night (Fig. 6B), suggesting that changes in phosphorylation were also not responsible for the diel variation observed in nitrate uptake. Several explanations can be advanced to account for this uptake rate variation. First, LpNRT2.1 may not be the only nitrate transporter in *Lingulodinium* contributing to nitrate uptake. A constitutively expressed LpNRT2.1 could be the main contributor to basal nitrate uptake at day and night, while other transporters, such as LpNRT2.2 and LpNRT2.3 could be induced by light. Second, an unknown interaction partner may be present and capable of stimulating LpNRT2.1 activity during the day, but not at night. Lastly, it was recently discovered that dinoflagellates have acquired by horizontal gene transfer from bacteria a suite of rhodopsins, including the light-driven proton pump proteorhodopsin (Slamovits et al., 2011). All characterized NRT2s are reported to be secondary active transporters coupling the transport of nitrate with that of protons, the H^+ gradient being generated by H^+-ATPase pumps (Fernandez and Galvan, 2007; Krapp et al., 2014). An intriguing possibility in *Lingulodinium* could be that proteorhodopsins are used as alternative to H^+-ATPases to generate the proton motive force necessary for nitrate transport by NRT2s. In this context,

Lingulodinium NRT2 activity would merely follow the light-regulated activity of proteorhodopsins, explaining the increased nitrate uptake observed during the day (Fig. 1A).

Circadian clocks are molecular systems that enable organisms to optimize their internal biochemistry in response to anticipated modifications in their environment. In *Lingulodinium*, there is circadian control of nitrate assimilation because the amount of NR in the cell is clock regulated with a maximum during the day (Ramalho et al., 1995). Maximum rates of nitrate reduction thus agree well with maximum rates of uptake measured here. It can be argued that light-dependent uptake is indirectly clock-controlled, as light intensity is higher at the surface and the diurnal vertical migration, which places *Lingulodinium* at the surface during the day, is a *bona fide* circadian rhythm (Roenneberg et al., 1989). The results presented here thus show that nitrate uptake is distinct from nitrate assimilation, as while nitrate reductase activity remains rhythmic in constant light, nitrate uptake does not.

5. Conclusion

This study provided a first glimpse of nitrate transporters in dinoflagellates and showed that global nitrate uptake in *Lingulodinium polyedrum* was driven by light rather than by a circadian clock. The LpNRT2 transporters were identified as the best candidates for nitrate uptake on the basis of sequence analysis, although their functional characterization in heterologous systems such as *Xenopus* oocytes will be necessary to confirm the role proposed here and to establish their kinetic properties. The approach presented here offers great promise for the identification of other transporters in dinoflagellates. Foremost amongst these are the ammonium, urea and phosphate transporters, which are all related to the formation and persistence of HABs.

Acknowledgements

Financial support from the Natural Sciences and Engineering Research Council of Canada (NSERC discovery grant 171382-03 to DM) and from the Fond de Recherche du Québec- Nature et Technologies (FQRNT) for a studentship (SDB) is gratefully acknowledged.

References

Anderson, D.M., Burkholder, J.M., Cochlan, W.P., Glibert, P.M., Gobler, C.J., Heil, C.A., Kudela, R., Parsons, M.L., Rensel, J.E., Townsend, D.W., Trainer, V.L., Vargo, G.A., 2008. Harmful algal blooms and eutrophication: Examining linkages from selected coastal regions of the United States. Harmful Algae 8(1), 39-53.

Anderson, D.M., Cembella, A.D., Hallegraeff, G.M., 2012. Progress in understanding harmful algal blooms: paradigm shifts and new technologies for research, monitoring, and management. Ann Rev Mar Sci 4, 143-176.

Beauchemin, M., Roy, S., Daoust, P., Dagenais-Bellefeuille, S., Bertomeu, T., Letourneau, L., Lang, B.F., Morse, D., 2012. Dinoflagellate tandem array gene transcripts are highly conserved and not polycistronic. Proc Natl Acad Sci U S A 109(39), 15793-15798.

Bergsdorf, E.-Y., Zdebik, A.A., Jentsch, T.J., 2009. Residues Important for Nitrate/Proton Coupling in Plant and Mammalian CLC Transporters. J Biol Chem 284(17), 11184-11193.

Bertomeu, T., Hastings, J.W., Morse, D., 2003. Vectorial labeling of dinoflagellate cell surface proteins. J Phycol 39(6), 1254-1260.

Bodeanu, N., Ruta, G., 1998. Development of the planktonic algae in the Romanian Black Sea sector in 1981-1996. Paris-Xunta de Galicia & Intergovernmental Oceanographic Commission of UNESCO, Paris, France.

Claros, M.G., von Heijne, G., 1994. TopPred II: an improved software for membrane protein structure predictions. Comput Appl Biosci 10(6), 685-686.

Clement, C.R., Hopper, M.J., Jones, L.H.P., Leafe, E.L., 1978. The Uptake of Nitrate by *Lolium perenne* from Flowing Nutrient Solution: II. EFFECT OF LIGHT, DEFOLIATION, AND RELATIONSHIP TO CO2 FLUX. J Exp Bot 29(5), 1173-1183.

Crawford, N.M., Forde, B.G., 2002. Molecular and developmental biology of inorganic nitrogen nutrition. *Arabidopsis* Book 1, e0011.

Dagenais Bellefeuille, S., Dorion, S., Rivoal, J., Morse, D., 2014. The dinoflagellate *Lingulodinium polyedrum* responds to N depletion by a polarized deposition of starch and lipid bodies. PLoS One 9 (11), e111067

Davy, S.K., Allemand, D., Weis, V.M., 2012. Cell Biology of Cnidarian-Dinoflagellate Symbiosis. Microbiol Mol Biol R 76(2), 229-261.

De Angeli, A., Monachello, D., Ephritikhine, G., Frachisse, J.M., Thomine, S., Gambale, F., Barbier-Brygoo, H., 2006. The nitrate/proton antiporter AtCLCa mediates nitrate accumulation in plant vacuoles. Nature 442(7105), 939-942.

Derelle, E., Ferraz, C., Rombauts, S., Rouze, P., Worden, A.Z., Robbens, S., Partensky, F., Degroeve, S., Echeynie, S., Cooke, R., Saeys, Y., Wuyts, J., Jabbari, K., Bowler, C., Panaud, O., Piegu, B., Ball, S.G., Ral, J.P., Bouget, F.Y., Piganeau, G., De Baets, B., Picard, A., Delseny, M., Demaille, J., Van de Peer, Y., Moreau, H., 2006. Genome analysis of the smallest free-living eukaryote *Ostreococcus tauri* unveils many unique features. Proc Natl Acad Sci U S A 103(31), 11647-11652.

Egge, J.K., 1998. Are diatoms poor competitors at low phosphate concentrations? J Marine Syst 16(3-4), 191-198.

Fernandez, E., Galvan, A., 2007. Inorganic nitrogen assimilation in Chlamydomonas. J Exp Bot 58(9), 2279-2287.

Forde, B.G., 2000. Nitrate transporters in plants: structure, function and regulation. BBA-Biomembranes 1465(1-2), 219-235.

Gasteiger, E., Gattiker, A., Hoogland, C., Ivanyi, I., Appel, R.D., Bairoch, A., 2003. ExPASy: the proteomics server for in-depth protein knowledge and analysis. Nucleic Acids Res 31(13), 3784-3788.

Geiger, D., Maierhofer, T., Al-Rasheid, K.A., Scherzer, S., Mumm, P., Liese, A., Ache, P., Wellmann, C., Marten, I., Grill, E., Romeis, T., Hedrich, R., 2011. Stomatal closure by fast abscisic acid signaling is mediated by the guard cell anion channel SLAH3 and the receptor RCAR1. Sci Signal 4(173), ra32.

Geiger, D., Scherzer, S.n., Mumm, P., Stange, A., Marten, I., Bauer, H., Ache, P., Matschi, S., Liese, A., Al-Rasheid, K.A.S., Romeis, T., Hedrich, R., 2009. Activity of guard cell anion channel SLAC1 is controlled by drought-stress signaling kinase-phosphatase pair. Proc Natl Acad Sci U S A 106(50), 21425-21430.

Glass, A.D., Britto, D.T., Kaiser, B.N., Kinghorn, J.R., Kronzucker, H.J., Kumar, A., Okamoto, M., Rawat, S., Siddiqi, M.Y., Unkles, S.E., Vidmar, J.J., 2002. The regulation of nitrate and ammonium transport systems in plants. J Exp Bot 53(370), 855-864.

Gruber, N., 2008. The Marine Nitrogen Cycle: Overview and Challenges, Nitrogen in the Marine Environment (2nd Edition). Academic Press, San Diego, pp. 1-50.

Harrison, W.G., 1976. Nitrate metabolism of the red tide dinoflagellate *Gonyaulax polyedra* Stein. J Exp Mar Biol Ecol 21(3), 199-209.

Hofmann, K., Stoffel, W., 1993. TMBASE- A database of membrane spanning protein segments Biol. Chem. 374, 166.

Huson, D.H., Scornavacca, C., 2012. Dendroscope 3: an interactive tool for rooted phylogenetic trees and networks. Syst Biol 61(6), 1061-1067.

Jentsch, T.J., 2008. CLC chloride channels and transporters: from genes to protein structure, pathology and physiology. Crit Rev Biochem Mol Biol 43(1), 3-36.

Kinghorn, J.R., Sloan, J., Kana'n, G.J.M., DaSilva, E.R., Rouch, D.A., Unkles, S.E., 2005. Missense Mutations That Inactivate the *Aspergillus nidulans* nrtA Gene Encoding a High-Affinity Nitrate Transporter. Genetics 169(3), 1369-1377.

Kotur, Z., Glass, A.D., 2015. A 150 kDa plasma membrane complex of AtNRT2.5 and AtNAR2.1 is the major contributor to constitutive high-affinity nitrate influx in *Arabidopsis thaliana*. Plant Cell Environ 38(8), 1490-1502.

Kotur, Z., Mackenzie, N., Ramesh, S., Tyerman, S.D., Kaiser, B.N., Glass, A.D., 2012. Nitrate transport capacity of the *Arabidopsis thaliana* NRT2 family members and their interactions with AtNAR2.1. New Phytol 194(3), 724-731.

Krapp, A., David, L.C., Chardin, C., Girin, T., Marmagne, A., Leprince, A.-S., Chaillou, S., Ferrario-Mery, S., Meyer, C., Daniel-Vedele, F.o., 2014. Nitrate transport and signalling in *Arabidopsis*. J Exp Bot 65(3), 789-798.

Krogh, A., Larsson, B., von Heijne, G., Sonnhammer, E.L., 2001. Predicting transmembrane protein topology with a hidden Markov model: application to complete genomes. J Mol Biol 305(3), 567-580.

Kudela, R.M., Cochlan, W.P., 2000. Nitrogen and carbon uptake kinetics and the influence of irradiance for a red tide bloom off southern California. Aquat Microb Ecol 21(1), 31-47.

Lejay, L., Tillard, P., Lepetit, M., Olive, F., Filleur, S., Daniel-Vedele, F., Gojon, A., 1999. Molecular and functional regulation of two NO_3^- uptake systems by N- and C-status of *Arabidopsis* plants. Plant J 18(5), 509-519.

Leran, S., Varala, K., Boyer, J.C., Chiurazzi, M., Crawford, N., Daniel-Vedele, F., David, L., Dickstein, R., Fernandez, E., Forde, B., Gassmann, W., Geiger, D., Gojon, A., Gong, J.M., Halkier, B.A., Harris, J.M., Hedrich, R., Limami, A.M., Rentsch, D., Seo, M., Tsay, Y.F., Zhang, M., Coruzzi, G., Lacombe, B., 2014. A unified nomenclature of NITRATE TRANSPORTER 1/PEPTIDE TRANSPORTER family members in plants. Trends Plant Sci 19(1), 5-9.

Lewis, J., Hallet, R., 1997. *Lingulodinium polyedrum* (*Gonyaulax polyedra*) a blooming dinoflagellate. Oceanogr Mar Biol Annu Rev 35, 97-161.

Lezhneva, L., Kiba, T., Feria-Bourrellier, A.B., Lafouge, F., Boutet-Mercey, S., Zoufan, P., Sakakibara, H., Daniel-Vedele, F., Krapp, A., 2014. The *Arabidopsis* nitrate transporter NRT2.5 plays a role in nitrate acquisition and remobilization in nitrogen-starved plants. Plant J 80(2), 230-241.

Macduff, J.H., Bakken, A.K., Dhanoa, M.S., 1997. An analysis of the physiological basis of commonality between diurnal patterns of NH_4^+, NO_3^- and K^+ uptake by *Phleum pratense* and *Festuca pratensis*. J Exp Bot 48(9), 1691-1701.

Matt, P., Geiger, M., Walch-Liu, P., Engels, C., Krapp, A., Stitt, M., 2001. The immediate cause of the diurnal changes of nitrogen metabolism in leaves of nitrate-replete tobacco: a major imbalance between the rate of nitrate reduction and the rates of nitrate uptake and ammonium metabolism during the first part of the light period. Plant Cell Environ 24(2), 177-190.

Miller, M.A., Pfeiffer, W., Schwartz, T., 2010. "Creating the CIPRES Science Gateway for inference of large phylogenetic trees", Proceedings of the Gateway Computing Environments Workshop (GCE), New Orleans, LA, pp. 1-8.

Moir, J.W., Wood, N.J., 2001. Nitrate and nitrite transport in bacteria. Cell Mol Life Sci 58(2), 215-224.

Nassoury, N., Cappadocia, M., Morse, D., 2003. Plastid ultrastructure defines the protein import pathway in dinoflagellates. J Cell Sci 116(Pt 14), 2867-2874.

Nassoury, N., Fritz, L., Morse, D., 2001. Circadian changes in ribulose-1,5-bisphosphate carboxylase/oxygenase distribution inside individual chloroplasts can account for the rhythm in dinoflagellate carbon fixation. Plant Cell 13(4), 923-934.

Okaichi, T., 1997. Red tides in the Seto Inland Sea. Terra Scientific Publishing Company, Tokyo, Japan.

Ono, F., Frommer, W.B., von Wirén, N., 2000. Coordinated Diurnal Regulation of Low- and High-Affinity Nitrate Transporters in Tomato. Plant Biol 2(1), 17-23.

Orsel, M., Chopin, F., Leleu, O., Smith, S.J., Krapp, A., Daniel-Vedele, F., Miller, A.J., 2006. Characterization of a two-component high-affinity nitrate uptake system in *Arabidopsis*. Physiology and protein-protein interaction. Plant Physiol 142(3), 1304-1317.

Peuke, A.D., Jeschke, W.D., 1998. The effects of light on induction, time courses, and kinetic patterns of net nitrate uptake in barley. Plant Cell Environ 21(8), 765-774.

Pierce, R.H., Henry, M.S., Blum, P.C., Lyons, J., Cheng, Y.S., Yazzie, D., Zhou, Y., 2003. Brevetoxin Concentrations in Marine Aerosol: Human Exposure Levels During a *Karenia brevis* Harmful Algal Bloom. B Environ Contam Tox 70(1), 161-165.

Ramalho, C.B., Hastings, J.W., Colepicolo, P., 1995. Circadian oscillation of nitrate reductase activity in *Gonyaulax polyedra* is due to changes in cellular protein levels. Plant Physiol 107(1), 225-231.

Roenneberg, T., Colfax, G.N., Hastings, J.W., 1989. A circadian rhythm of population behavior in *Gonyaulax polyedra*. J Biol Rhythms 4(2), 201-216.

Roenneberg, T., Rehman, J., 1996. Nitrate, a nonphotic signal for the circadian system. FASEB J 10(12), 1443-1447.

Roy, S., Beauchemin, M., Dagenais-Bellefeuille, S., Letourneau, L., Cappadocia, M., Morse, D., 2014a. The *Lingulodinium* circadian system lacks rhythmic changes in transcript abundance. BMC Biol 12, 107.

Roy, S., Letourneau, L., Morse, D., 2014b. Cold-induced cysts of the photosynthetic dinoflagellate *Lingulodinium polyedrum* have an arrested circadian bioluminescence rhythm and lower levels of protein phosphorylation. Plant Physiol 164(2), 966-977.

Slamovits, C.H., Okamoto, N., Burri, L., James, E.R., Keeling, P.J., 2011. A bacterial proteorhodopsin proton pump in marine eukaryotes. Nat Commun 2, 183.

Slot, J.C., Hallstrom, K.N., Matheny, P.B., Hibbett, D.S., 2007. Diversification of NRT2 and the Origin of Its Fungal Homolog. Mol Biol Evol 24(8), 1731-1743.

Smayda, T.J., 1997. Harmful algal blooms: their ecophysiology and general relevance to phytoplankton blooms in the sea. Limnol Oceanogr 42, 1137-1153

Stamatakis, A., 2014. RAxML version 8: a tool for phylogenetic analysis and post-analysis of large phylogenies. Bioinformatics 30(9), 1312-1313.

Trueman, L.J., Richardson, A., Forde, B.G., 1996. Molecular cloning of higher plant homologues of the high-affinity nitrate transporters of *Chlamydomonas reinhardtii* and *Aspergillus nidulans*. Gene 175(1-2), 223-231.

Tsay, Y.F., Chiu, C.C., Tsai, C.B., Ho, C.H., Hsu, P.K., 2007. Nitrate transporters and peptide transporters. FEBS Lett 581(12), 2290-2300.

Unkles, S.E., Hawker, K.L., Grieve, C., Campbell, E.I., Montague, P., Kinghorn, J.R., 1991. crnA encodes a nitrate transporter in *Aspergillus nidulans*. Proc Natl Acad Sci U S A 88(1), 204-208.

Unkles, S.E., Karabika, E., Symington, V.F., Cecile, J.L., Rouch, D.A., Akhtar, N., Cromer, B.A., Kinghorn, J.R., 2012. Alanine scanning mutagenesis of a high-affinity nitrate transporter highlights the requirement for glycine and asparagine residues in the two nitrate signature motifs. Biochem J 447(1), 35-42.

Unkles, S.E., Rouch, D.A., Wang, Y., Siddiqi, M.Y., Glass, A.D., Kinghorn, J.R., 2004. Two perfectly conserved arginine residues are required for substrate binding in a high-affinity nitrate transporter. Proc Natl Acad Sci U S A 101(50), 17549-17554.

Unkles, S.E., Zhou, D., Siddiqi, M.Y., Kinghorn, J.R., Glass, A.D., 2001. Apparent genetic redundancy facilitates ecological plasticity for nitrate transport. EMBO J 20(22), 6246-6255.

von der Fecht-Bartenbach, J., Bogner, M., Dynowski, M., Ludewig, U., 2010. CLC-b-Mediated NO_3^-/H^+ Exchange Across the Tonoplast of *Arabidopsis* Vacuoles. Plant and Cell Physiology 51(6), 960-968.

von Heijne, G., 1992. Membrane protein structure prediction. Hydrophobicity analysis and the positive-inside rule. J Mol Biol 225(2), 487-494.

Wang, R., Xing, X., Crawford, N., 2007. Nitrite Acts as a Transcriptome Signal at Micromolar Concentrations in *Arabidopsis* Roots. Plant Physiol 145(4), 1735-1745.

Wege, S., Jossier, M., Filleur, S., Thomine, S., Barbier-Brygoo, H., Gambale, F., De Angeli, A., 2010. The proline 160 in the selectivity filter of the *Arabidopsis* NO_3^-/H^+ exchanger AtCLCa is essential for nitrate accumulation in planta. Plant J 63(5), 861-869.

Zhou, J.-J., Fernandez, E., Galvan, A., Miller, A.J., 2000a. A high affinity nitrate transport system from Chlamydomonas requires two gene products. FEBS Letters 466(2,Äì3), 225-227.

Zhou, J.J., Trueman, L.J., Boorer, K.J., Theodoulou, F.L., Forde, B.G., Miller, A.J., 2000b. A high affinity fungal nitrate carrier with two transport mechanisms. J Biol Chem 275(51), 39894-39899.

Zhou, M.-j., Shen, Z.-l., Yu, R.-c., 2008. Responses of a coastal phytoplankton community to increased nutrient input from the Changjiang (Yangtze) River. Cont Shelf Res 28(12), 1483-1489.

Figure legends

Figure 1: Nitrate uptake in *Lingulodinium* is light dependent. A) Daily and B) circadian uptake measured as $\delta^{15}N$. Results are mean ± SE (n=3). Statistically different results ($p < 0.05$) are marked with a different letter (Analysis of variance). Data presented in B) are not statistically different. ZT; Zeitgeber time, CT; Circadian time.

Figure 2: Transcripts of NRT2.1 are the most abundant, relative to all of *Lingulodinium* putative nitrate transporter sequences. RPKM data for putative nitrate transporters from table 1 (A to W) were generated after mapping raw reads onto a Trinity assembly. Bars are: A; LpNRT2.1 (GABP01091661), B; LpNRT2.2 (JO755411), C; LpNRT2.3 (GABP01019652), D; JO716588, E; JO704794, F; GABP01017364, G; GABP01007646, H; GABP01067085, I; GABP01030193, J; GABP01023136, K; GABP01020755, L; GABP01013780, M; GABP01037384, N; GABP01029549, O; GABP01035949, P; GABP01073801, Q; GABP01068566, R; GABP01106673, S; GABP01044984, T; GABP01064559, U; GABP01053663, V; JO745918, W; GABP01000849. Results are mean ± SE (n=8). Statistically different results ($p < 0.05$) are marked over the bars with a different lower case letter (Analysis of variance). RPKM; Reads Per Kilobase per Million.

Figure 3: *Lingulodinium* NRT2 sequences are found in two different clades. Maximum-likelihood tree of NRT2 sequences as reconstructed by RAxML. *Lingulodinium* sequences, in bold characters, are found in a well-supported dinoflagellate-specific clade as well as in a clade formed primarily of green algal sequences.

Figure 4: All sites essential for nitrate transport are conserved in *Lingulodinium* NRT2 sequences. NRT2 sequences were aligned and compared to the NrtA of *Aspergillus nidulans*, in which mutagenesis studies have defined the residues required for nitrate transport. Only the regions where these sites (boxes) are localized are presented in the alignment. Two nitrate signature regions, NS1 and NS2, were further marked because they each contained the NRT2 specific motif. There are two and four mismatches to the canonical motif in NS1 and NS2, respectively. The G after the dashed line in NS1 was not included in the motif, but is essential for nitrate transport. F47; Phe^{47} of *A. nidulans* NrtA, R87 and R368; Arg^{87} and Arg^{368} of *A. nidulans* NrtA, N168 and N459; Asn^{168} and Asn^{459} of *Aspergillus* NrtA.

Figure 5: Mature dinoflagellate NRT2 share the 12 predicted transmembrane domains. NrtA from *Aspergillus* and NRT2.5 from *Arabidopsis* were compared to the NRT2 sequences of the dinoflagellates, *Symbiodinium*, *Alexandrium* and *Lingulodinium*. All sequences were submitted to TMHMM, TMPred and TopPred and a summary of their analysis is presented. Domains, which were either undetected or below the default threshold in one of the predictors, but detected in others, were marked as "Putative TM". The $N_{cytosolic}$: $C_{cytosolic}$ topology prediction of TMPred and TopPred was selected for presentation, because both predictors shared the same results for all sequences analysed. Corresponding positions for F47, R87, R368, NS1 and NS2 of *Aspergillus* NrtA to the other sequences were followed with dashed lines. R87 and R368 ; Arg^{87} and Arg^{368} of *A. nidulans* NrtA, NS ; Nitrate Signature, An ; *A. nidulans*, At ; *A. thaliana*, Ata ; *A. tamarense*, Ssp ; *Symbiodinium* sp. Freudenthal, Lp ; *L. polyedrum*

Figure 6: LpNRT2.1 is constitutively expressed. Western blot analyses of LpNRT2.1 on 1D gels (A, C) or on 2D gels (B). Samples were taken at the indicated times over a daily cycle in

normal f/2 medium (A, B) or after 2 h or 24 h growth in medium containing the indicated N source. Rubisco was used as a loading control. Rub; Rubisco, +NO_3^-; normal f/2 supplemented with 880 µM NO_3^-, +$NO2^-$; f/2 with 10 µM and no nitrate, +NH_4^+; f/2 with 40 µM NH_4^+ and no nitrate, -N; f/2 lacking added N, ZT; Zeitgeber time

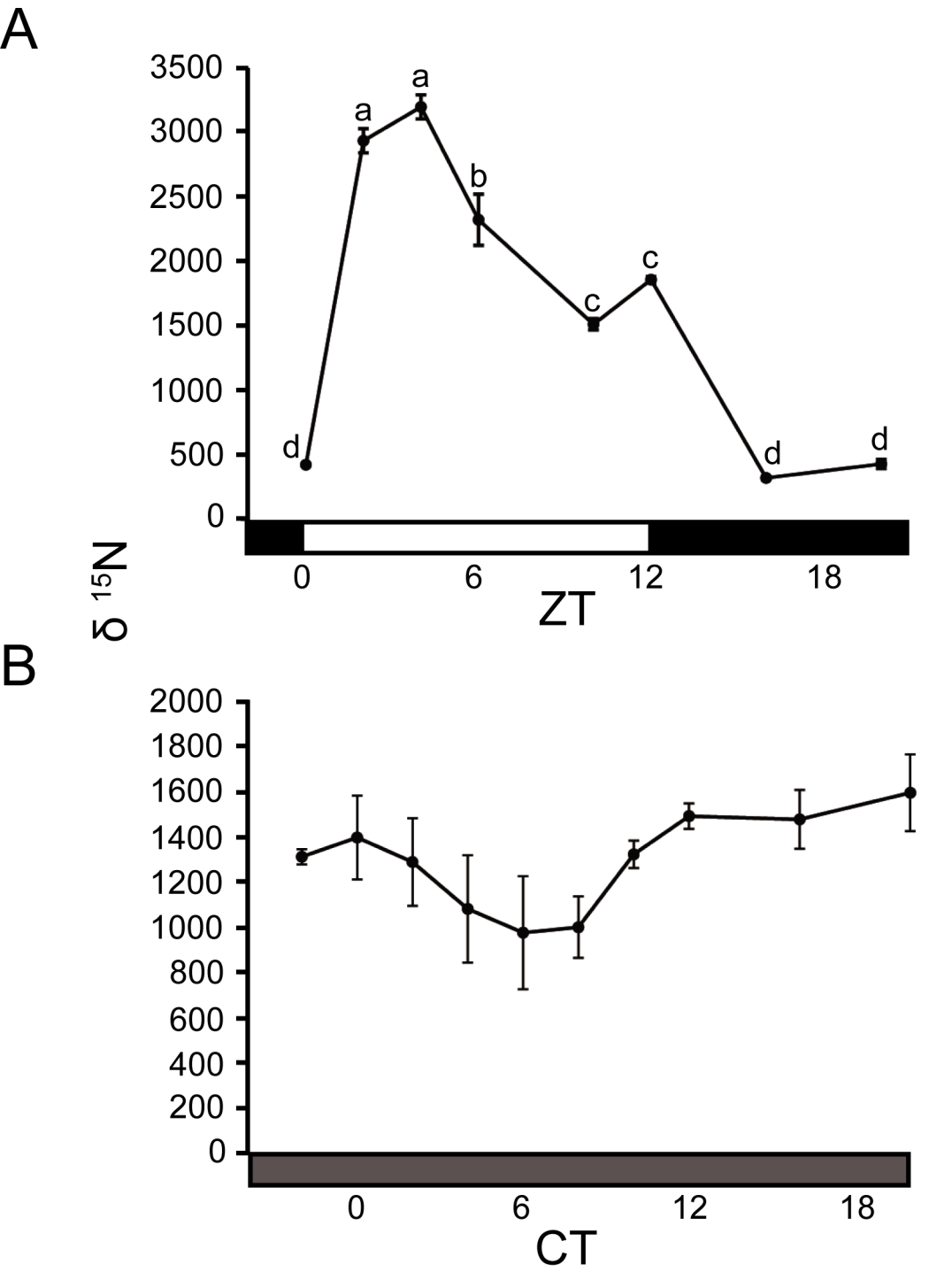
A
3500
3000
2500
2000
1500
1000
500
0
a
a
b
c
c
d
d
d
δ 15N
0
6
12
18
ZT
B
2000
1800
1600
1400
1200
1000
800
600
400
200
0
0
6
12
18
CT

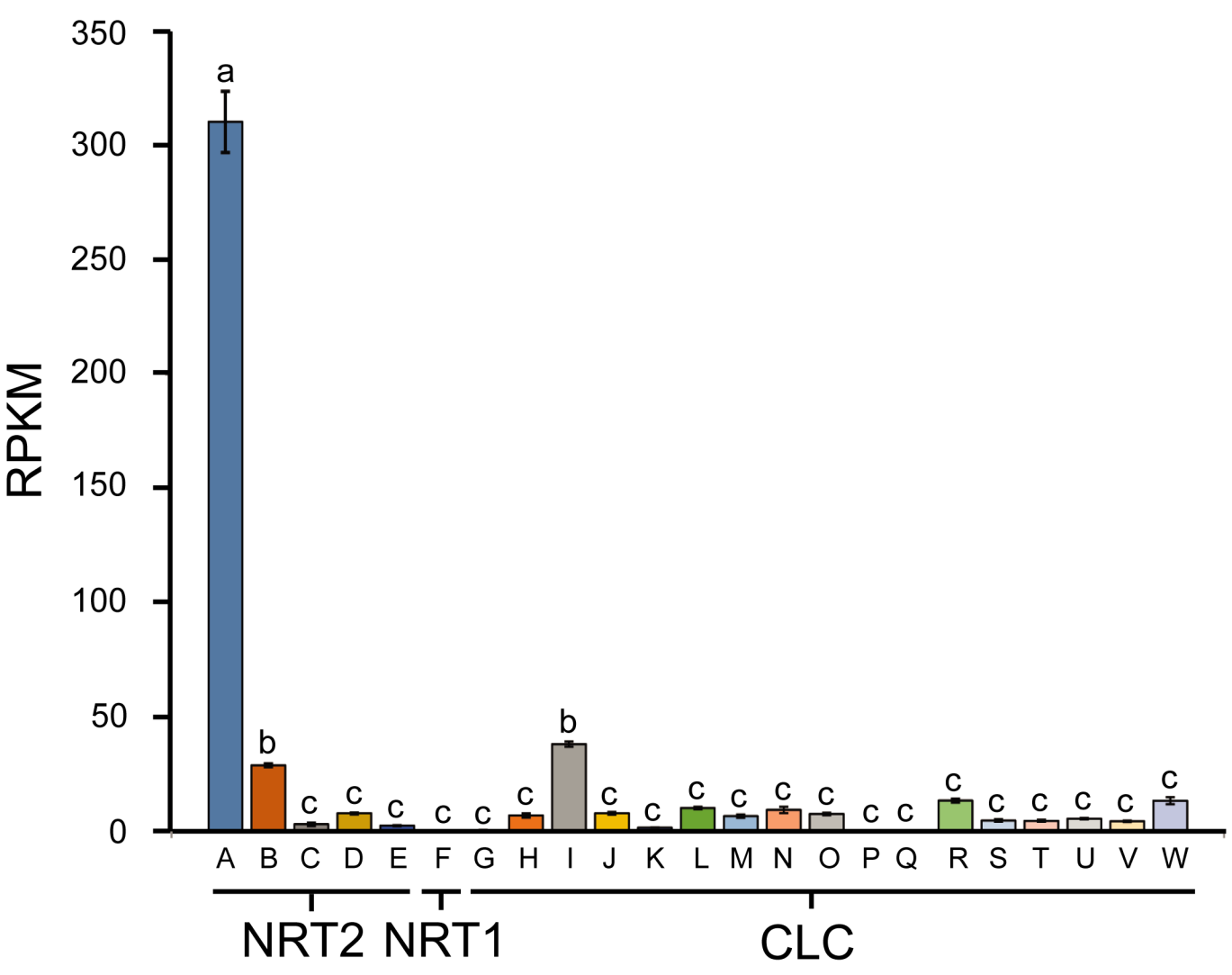
RPKM
350
300
250
200
150
100
50
0
a
b
c
c
c
c
c
c
b
c
c
c
c
c
c
c
c
c
c
c
c
c
c
c
A B C D E F G H I J K L M N O P Q R S T U V W
NRT2
NRT1
CLC

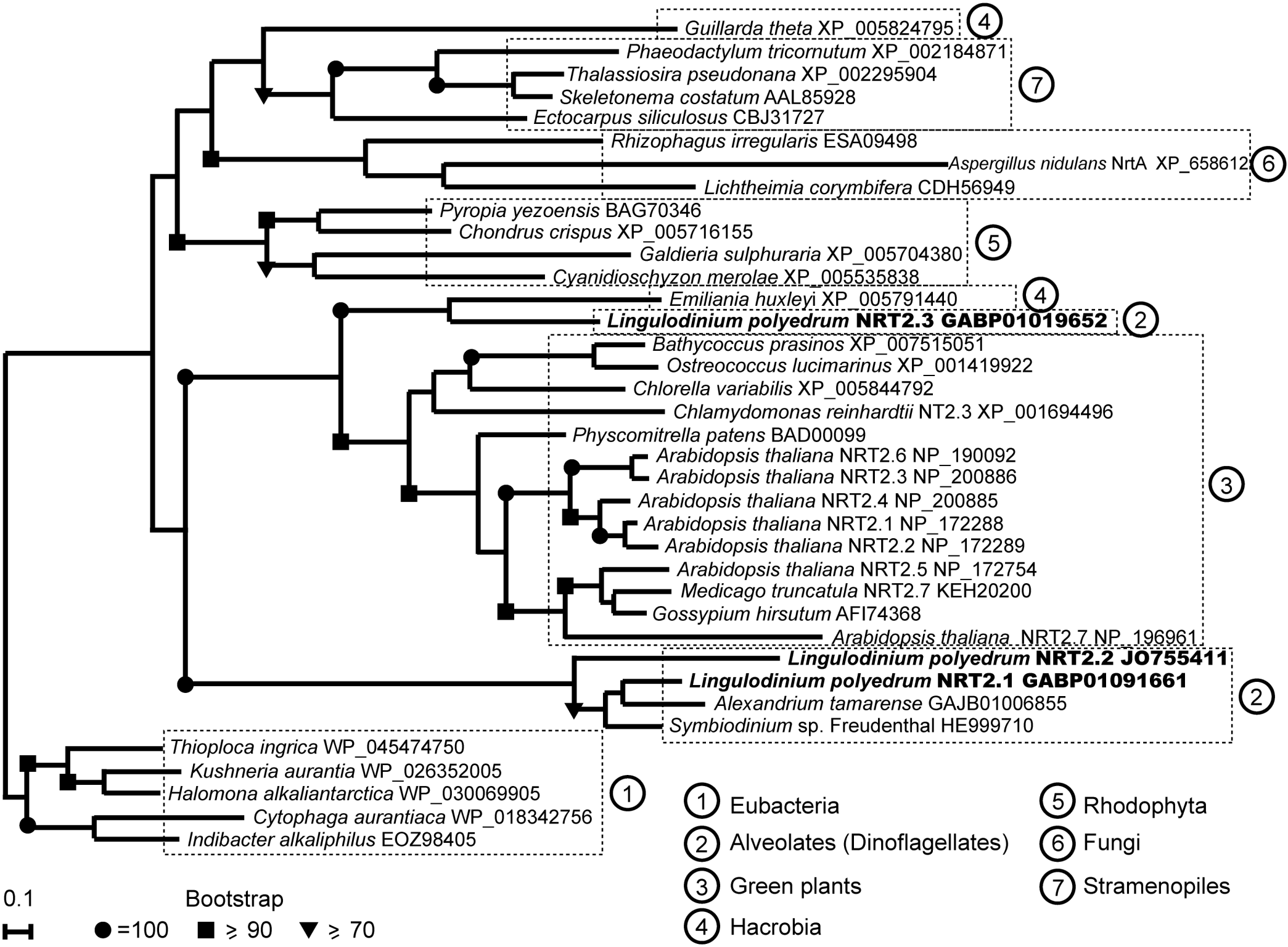
Guillarda theta XP_005824795
Phaeodactylum tricornutum XP_002184871
Thalassiosira pseudonana XP_002295904
Skeletonema costatum AAL85928
Ectocarpus siliculosus CBJ31727
Rhizophagus irregularis ESA09498
Aspergillus nidulans NrtA XP_658612
Lichtheimia corymbifera CDH56949
Pyropia yezoensis BAG70346
Chondrus crispus XP_005716155
Galdieria sulphuraria XP_005704380
Cyanidioschyzon merolae XP_005535838
Emiliania huxleyi XP_005791440
Lingulodinium polyedrum NRT2.3 GABP01019652
Bathycoccus prasinos XP_007515051
Ostreococcus lucimarinus XP_001419922
Chlorella variabilis XP_005844792
Chlamydomonas reinhardtii NT2.3 XP_001694496
Physcomitrella patens BAD00099
Arabidopsis thaliana NRT2.6 NP_190092
Arabidopsis thaliana NRT2.3 NP_200886
Arabidopsis thaliana NRT2.4 NP_200885
Arabidopsis thaliana NRT2.1 NP_172288
Arabidopsis thaliana NRT2.2 NP_172289
Arabidopsis thaliana NRT2.5 NP_172754
Medicago truncatula NRT2.7 KEH20200
Gossypium hirsutum AFI74368
Arabidopsis thaliana NRT2.7 NP_196961
Lingulodinium polyedrum NRT2.2 JO755411
Lingulodinium polyedrum NRT2.1 GABP01091661
Alexandrium tamarense GAJB01006855
Symbiodinium sp. Freudenthal HE999710
Thioploca ingrica WP_045474750
Kushneria aurantia WP_026352005
Halomona alkaliantarctica WP_030069905
Cytophaga aurantiaca WP_018342756
Indibacter alkaliphilus EOZ98405
4
7
6
5
4
2
3
2
1
0.1
Bootstrap
=100
≥ 90
≥ 70
1 Eubacteria
2 Alveolates (Dinoflagellates)
3 Green plants
4 Hacrobia
5 Rhodophyta
6 Fungi
7 Stramenopiles

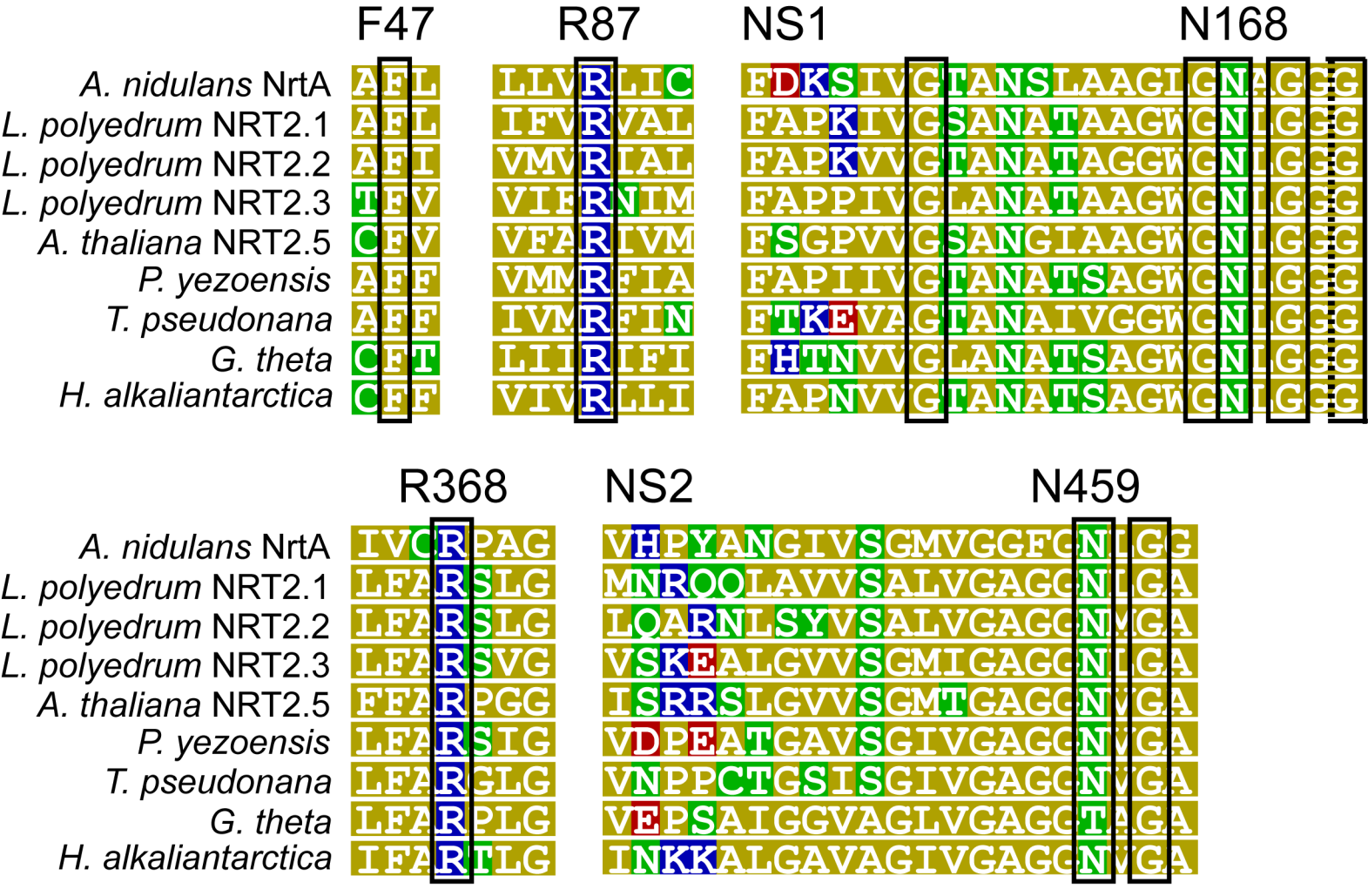
F47
R87
NS1
N168
A. nidulans NrtA
L. polyedrum NRT2.1
L. polyedrum NRT2.2
L. polyedrum NRT2.3
A. thaliana NRT2.5
P. yezoensis
T. pseudonana
G. theta
H. alkaliantarctica
R368
NS2
N459

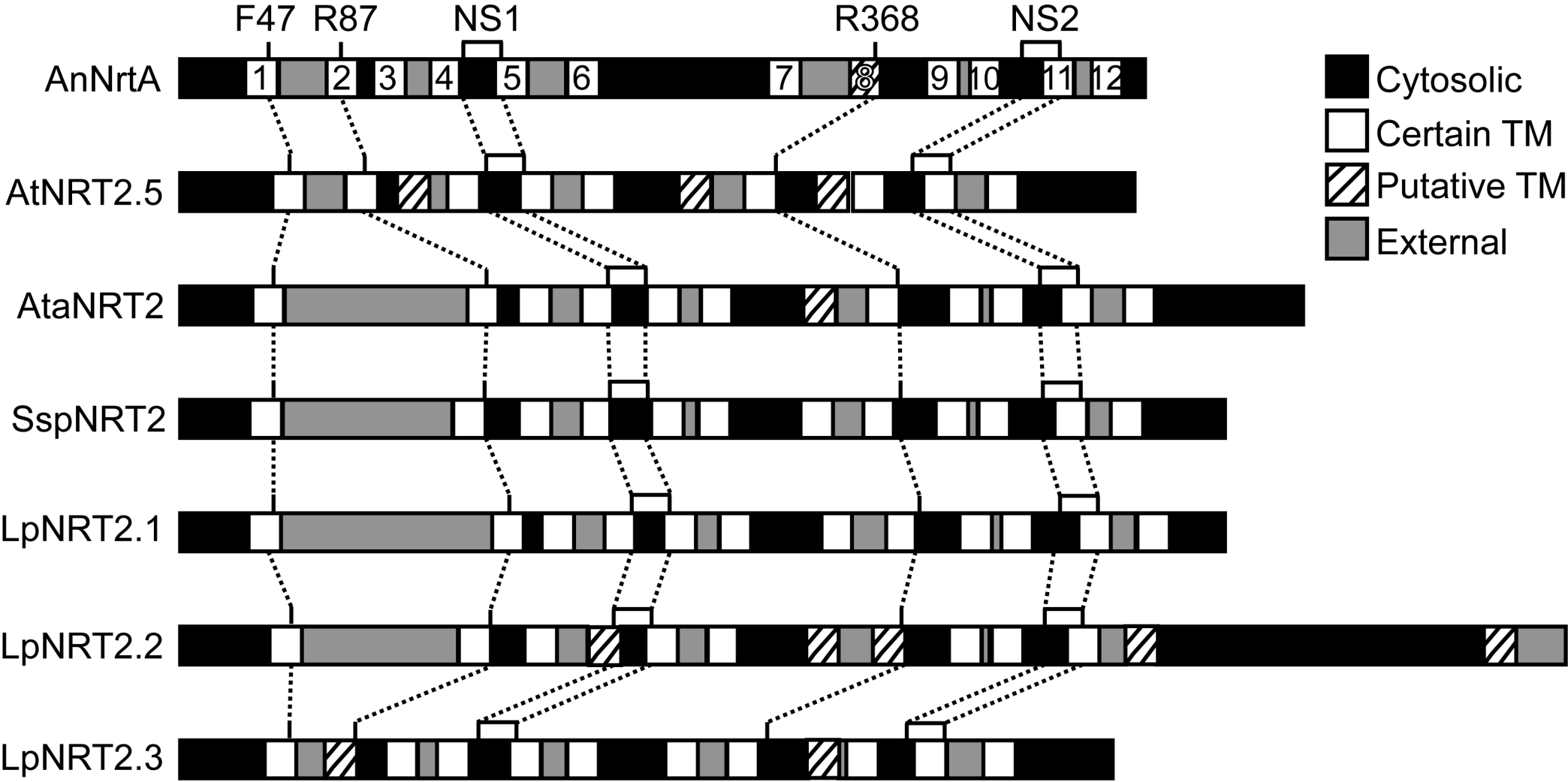
F47
R87
NS1
R368
NS2
AnNrtA
1
2
3
4
5
6
7
8
9
10
11
12
AtNRT2.5
AtaNRT2
SspNRT2
LpNRT2.1
LpNRT2.2
LpNRT2.3
Cytosolic
Certain TM
Putative TM
External

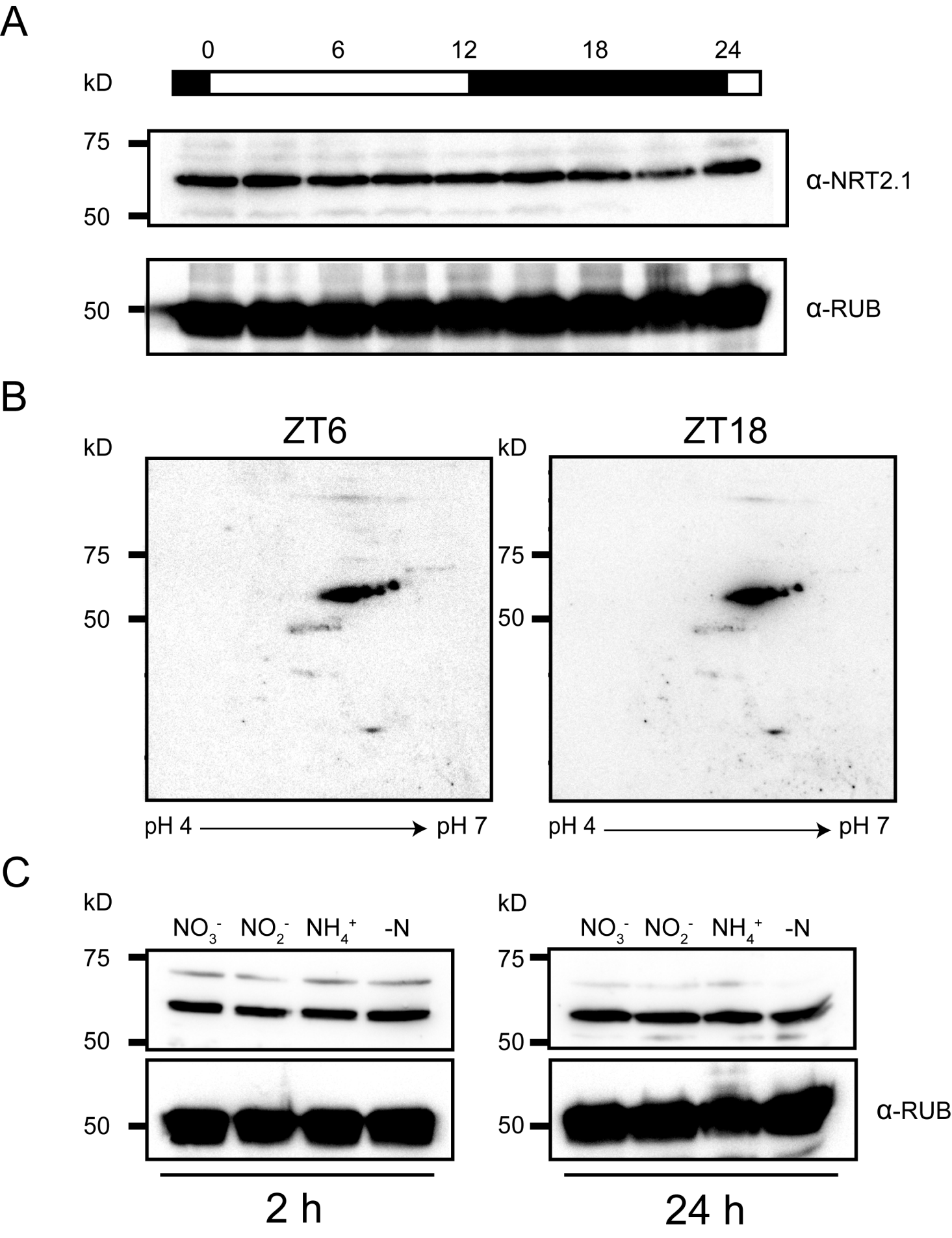
A
0
6
12
18
24
kD
75
50
α-NRT2.1
50
α-RUB
B
ZT6
ZT18
kD
75
50
pH 4
pH 7
C
NO_3^- NO_2^- NH_4^+ -N
2 h
24 h

Based on the comments I have received from the Editorial Board and my own read of the paper, I will accept it pending suitable revision. It was also pointed out to me that one reviewer said they "would typically expect to see a manuscript such as this in a different journal, such as J. Phycology. The paper is solid, and L. polyedrum can certainly be considered an HAB, but this is more of a description of N-transporters in a dinoflagellate, rather than a paper describing an HAB species".

Please be sure that the entire paper is in the third person (Clearly noted in the instructions to authors) - no I, we, or our.

Corrected

Do not begin sentences with any abbreviations, Latin names or 'however'.

Corrected

The figures also need attention and are not drawn according to the instructions. Figure 1 and all others - Arial font - and put the A and B On the panel, upper left. The whole idea of having A and B is to combine figures, so only needs one Y axis label - centered.

Corrected

Figure 3 appears to be color printed as black and white and that will not work. all of the key 'dots' are the same shade of gray!

Corrected

Figure 4 is not high resolution and all of the Latin names need to be in italics.

Corrected

Figure 5, the shading needs to be better differentiated and the key can go in the upper right portion of the graph, not at the bottom like a label. Anything that you plan to print in color on the internet needs to be

clear in the black and white printed version and all features discernible.

Corrected

- This manuscript presents a series of experiments describing nitrate transporters in L. polyedrum. There's not much known about these transporters (in dinoflagellates), and there are obvious implications for the ecophysiology of L. polyedrum and other dinoflagellates. The paper is generally very well written, and the experimental evidence provides good support for their conclusions. As I was reading the ms. some questions came to mind, such as the potential for undescribed transporters and for post-translational modification, but the discussion section brings those up and includes a nice discussion about the implications.

I generally agree that the authors have demonstrated convincing evidence that NRT2 is at least a common transporter, with the possibility of others also being present. And their culture studies do suggest that it is constitutive. Given that the target audience is the readership of Harmful Algae, I think they could expand a bit on where L. polyedrum fits, by briefly discussing (a la Smayda) what grouping of dinoflagellate it falls into, since I think that is relevant to the apparent constitutive uptake capacity for nitrate.

We have now added a paragraph to the discussion that treats the three classes of dinoflagellate described by Smayda (1997 Limnol Ocean 42:1137) (Affinity Strategy, Growth Strategy, Storage strategy).

A few minor comments are below. I would like to see these addressed before the manuscript is published, but I don't see any serious issues that would present this work from being accepted.

Section 2.1.3. This can be confusing, because f/2 already has 880 µM nitrate. I assume when the authors say f/2+NH4 and f/2+NO2 they mean N-deplete f/2 was supplemented with 40 and 10 µM N respectively, and not that f/2 with 880 µM nitrate was supplemented with NO2 or NH4. It would help to clarify that.

This has been clarified in methods

Results: while del-15N is probably fine for looking at relative patterns, it is more common in the literature to calculate V or Rho, since that accounts for ambient nutrient concentrations, time, etc. Do the patterns change when you use that, instead of looking at enrichment? Also, what was the natural abundance value for the cultures?

We did not calculate V since the amount of 15N used as a source was too high to be measured by the commercial facility. We note that since the source value is high, the deltaN values are proportional to V (ie. when Rsource>>Rsample in the following formula):

$$Vt = \frac{(Rsample - na)}{(Rsource - Rsample)\,\Delta T}$$

The d15N of untreated cells (natural abundance) was low, as expected (-5.6 ± 0.1).

Results: did you try running CT experiments after multiple days in constant light? If it were a circadian clock (which I agree it does not look like) that often "drifts" with time.

No, the rhythms usually dampen out over time (due to desynchronization) making the first few LL periods the easiest to find rhythms.

Supplementary Figure 1: del-15N is not the same as calculating an uptake rate (see other comment)

This has been changed to "absolute 15N enrichment".

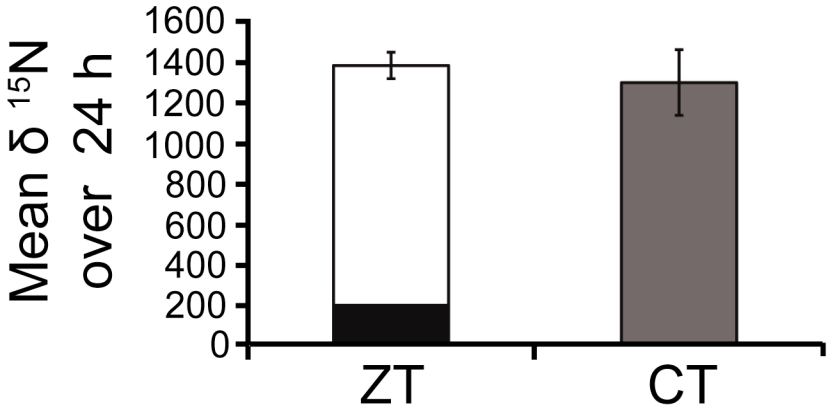

Supplementary figure 1: Absolute ^{15}N enrichment in *Lingulodinium* is the same over a 24 h period in ZT or CT. Mean δ ^{15}N was obtained by combining data from Fig. 1A and 1B. Values for ZT were calculated by adding the means of δ ^{15}N in the light (white bar) and dark (black bar) phases divided by 2 to account for the difference in uptake observed between day and night. Values for CT were calculated by taking the mean of all time points in B). Results are mean ± SE (n=3). Data are not statistically different. ZT; Zeitgeber time, CT; Circadian time.

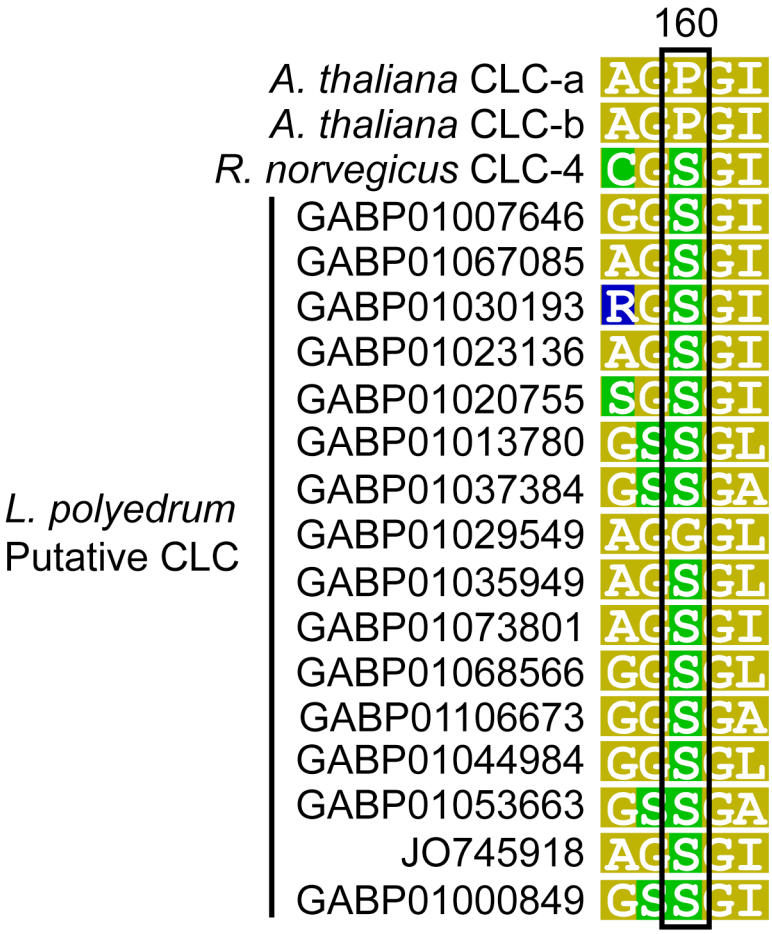

Supplementary figure 2: *Lingulodinium* putative CLC are predicted to be unselective for nitrate. *Lingulodinium polyedrum* putative CLC (see table 1) were compared to *Arabidopsis thaliana* CLC-a and CLC-b, and *Rattus norvegicus* CLC-4. Position 160 from *Arabidopsis* CLC-a indicated the position of the selectivity filter. Instead of a proline residue found in plant and reported to be essential for nitrate selectivity, mammalian and all except one dinoflagellate sequences contain a serine residue, typically found in chloride specialized transporters.

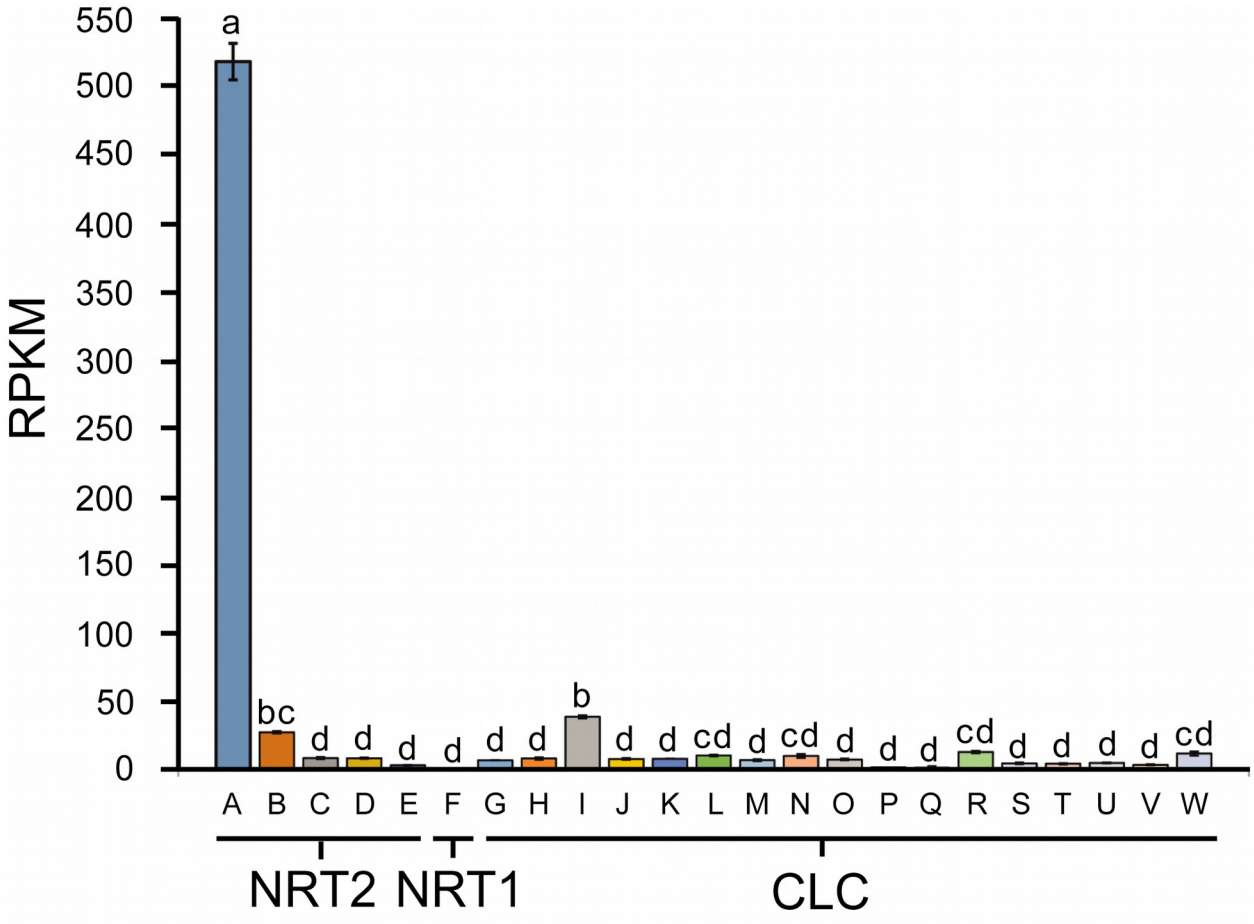

Supplementary figure 3: Transcripts of NRT2.1 are the most abundant, relative to all of *Lingulodinium* putative nitrate transporter sequences. RPKM data for putative nitrate transporters from table 1 (A to W) were generated after mapping raw reads onto a Velvet assembly. Bars are: A; LpNRT2.1_GABP01091661, B; LpNRT2.2_JO755411, C; LpNRT2.3_GABP01019652, D; JO716588, E; JO704794, F; GABP01017364, G; GABP01007646, H; GABP01067085, I; GABP01030193, J; GABP01023136, K; GABP01020755, L; GABP01013780, M; GABP01037384, N; GABP01029549, O; GABP01035949, P; GABP01073801, Q; GABP01068566, R; GABP01106673, S; GABP01044984, T; GABP01064559, U; GABP01053663, V; JO745918, W; GABP01000849. Results are mean ± SE (n=8). Statistically different results ($p < 0.05$) are marked over the bars with a different lower case letter (Analysis of variance). RPKM; Reads Per Kilobase per Million

Table 1| BLAST searches for putative nitrate transporters in *Lingulodinium polyedrum*

Query name	Hits ≤ e^{-20}	Unique sequences	Accession
AtNRT2.1	11	5	GABP01091661; JO755411; GABP01019652; JO716588; JO704794
AtNAR2.1	0	0	-
AtNPF6.3 (CHL1)	1	1	GABP01017364
AtCLC-a	36	17	GABP01007646; GABP01067085; GABP01030193; GABP01023136; GABP01020755; GABP01013780; GABP01037384; GABP01029549; GABP01035949; GABP01073801; GABP01068566; GABP01106673; GABP01044984; GABP01064559; GABP01053663; JO745918; GABP01000849
AtSLAC1	0	0	-